

**Supporting Information for:**

**Spin-orbit coupling prevents spin channel  
suppression upon transition metal atoms on  
armchair graphene nanoribbons**

W. Y. Rojas,<sup>†</sup> Cesar E. P. Villegas,<sup>‡</sup> and A.R. Rocha<sup>¶</sup>

<sup>†</sup>*School of Electronic Engineering, Bangor University, Bangor LL57 1UT, UK.; Centro de Ciências Naturais e Humanas, Universidade Federal do ABC, Santo André, Brazil.*

<sup>‡</sup>*Departamento de Ciencias, Universidad Privada del Norte, Av. Andrés Belaunde cdra 10 s/n, Comas, Lima, Peru*

<sup>¶</sup>*Instituto de Física Teórica, Universidade Estadual Paulista (UNESP), Rua Dr. Bento T. Ferraz, 271, São Paulo, SP 01140-070, Brazil.*

E-mail:

# Density of states of states for stable structure: Ir adatom

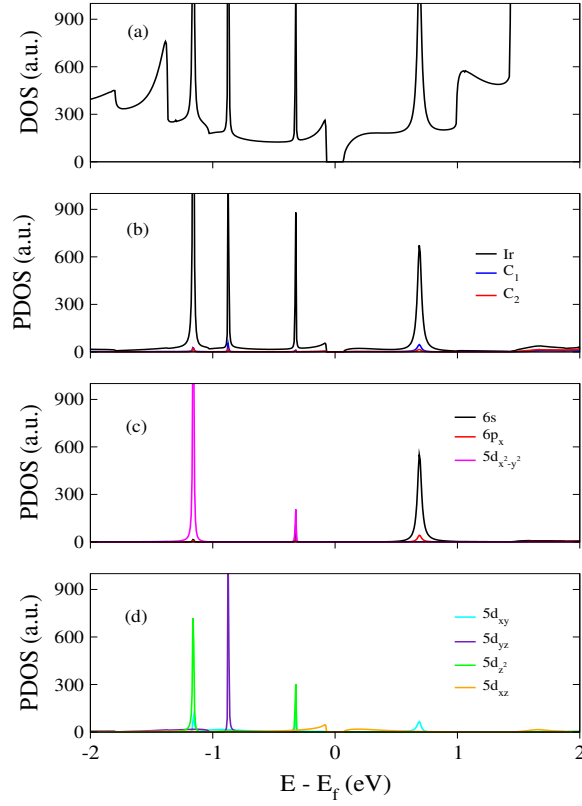


Figure S1: For Ir@AGNR-s : (a) Total DOS. (b) PDOS for Ir as well as C<sub>1</sub> and C<sub>2</sub> carbons atoms that are shown in the main text (Figure 1). (c) PDOS of 6s, 6p<sub>x</sub> and 5d orbitals of Ir. (d) PDOS of 5d orbitals of Ir.

Figure S1-(a) shows the density of states for the stable structure, Ir@AGNR-s. In figure S1-(b) it is depicted the projected density of states for Ir and selected carbon atoms. Our results also shows that the strong localized states in the valence band corresponds mostly to 5d orbitals of Ir whereas the most contribution in the conduction bands corresponds to 6s Ir orbitals.

## Density of states for symmetric structure: Ir adatom

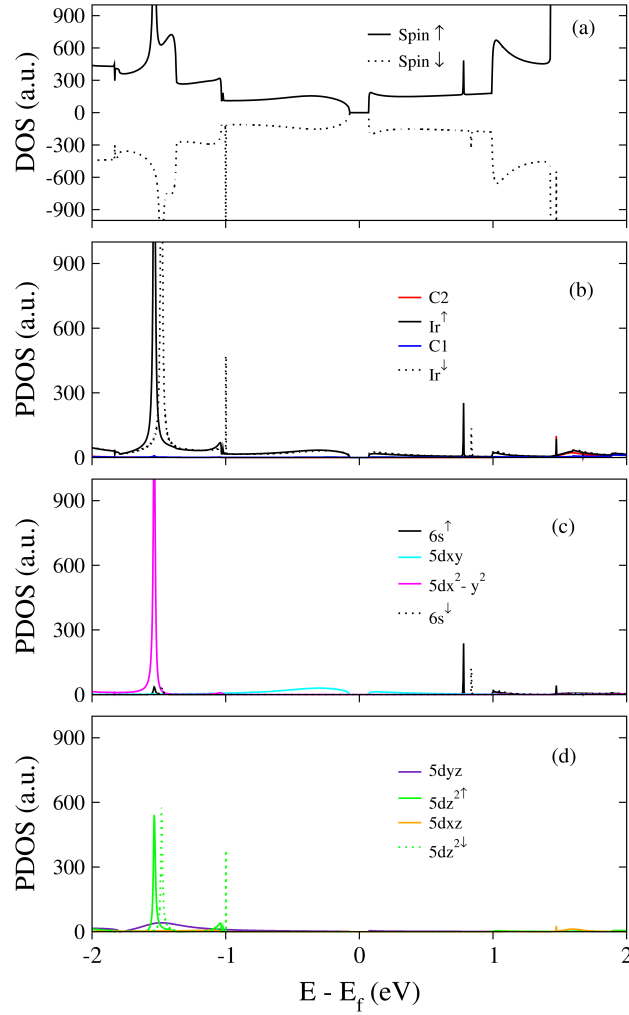


Figure S2: For Ir@AGNR-sy : (a) Total DOS. (b) PDOS of Ir and carbons  $C_1$  and  $C_2$ . (c) PDOS of  $6s$  and  $5d$  orbitals of Ir. (d) PDOS of  $5d$  orbitals of Ir.

In Fig. S2-(a) shows the density of states for the symmetric structure, Ir@AGNR-sy, including the spin degree of freedom. In contrast to the stable case, the stronger localized states are observed in the conduction band arising from  $6s$  Ir atoms whereas in the valence band dominates localized states coming from  $5d$  orbitals (Fig. S2- (c-d))

# PDOS and spin-flip transmission probabilities for Ni adatom: Stable structure

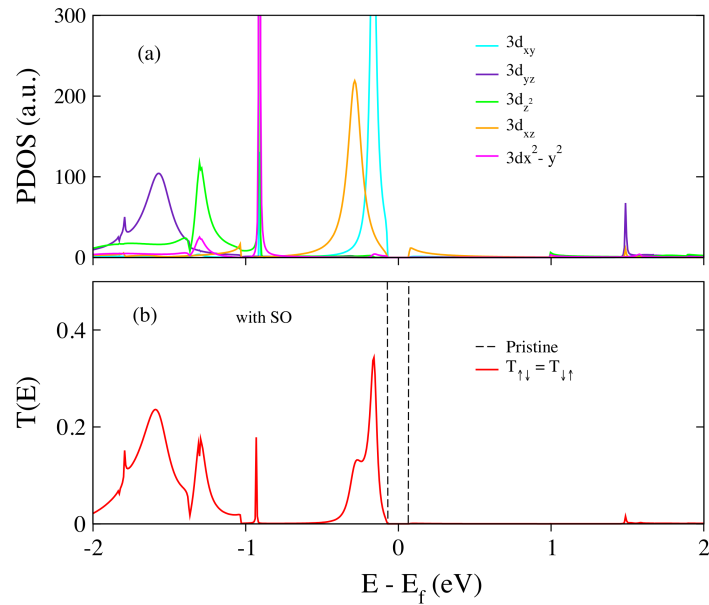


Figure S3: For Ni@AGNR-s : (a) PDOS of 3d orbitals of Ni. (b) Spin-flip transmission coefficients.

In Fig. S3 we present a zoom in of the (a) PDOS and its corresponding (b) transmission coefficients of spin-flip degree of freedom. In this way, we highlight the relation between the local impurity resonances with the energy states.

# PDOS and spin-flip transmission probabilities for Ni adatom: Symmetric structure

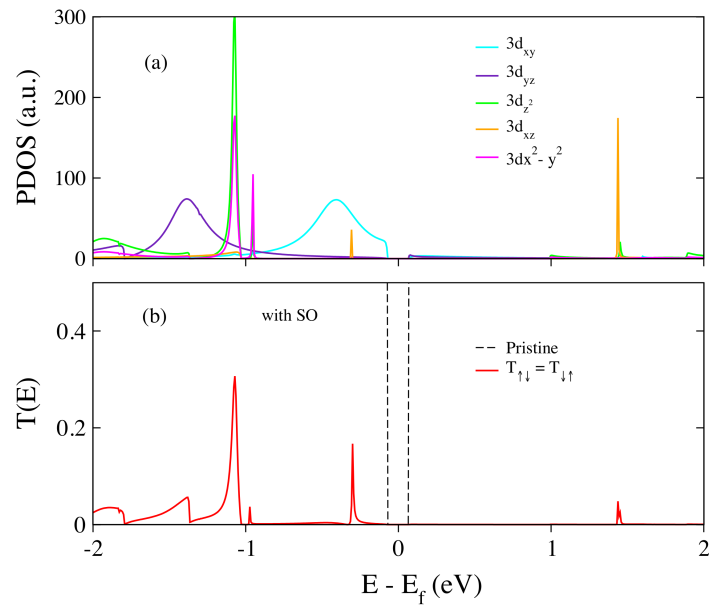


Figure S4: For Ni@AGNR-sy : (a) PDOS of 3d orbitals of Ni. (b) Spin-flip transmission coefficients.

In Fig. S4 we present a zoom in of the (a) PDOS and its corresponding (b) transmission coefficients of spin-flip degree of freedom. In this way, we emphasize the relation between the local impurity resonances with the energy states.

# PDOS and spin-flip transmission probabilities for Ir adatom:

## Stable structure

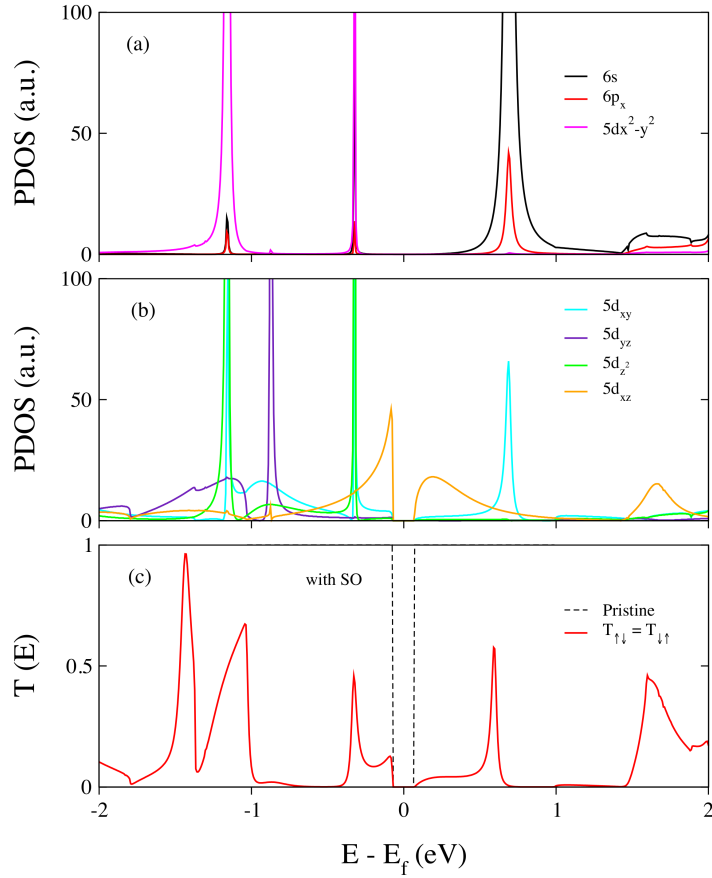


Figure S5: For Ir@AGNR-s : (a)-(b) PDOS of  $6s$ ,  $6px$ , and  $5d$  orbitals of Ir. (c) Spin-flip transmission coefficients.

Fig. S5 shows a zoom in of the PDOS for (a)  $6s$ ;  $6px$  and (b)  $5d$  orbitals of Ir. The transmission coefficients are also shown in chart (c) to highlight the eventual relation between the local impurity resonances with the energy states.

# PDOS and spin-flip transmission probabilities for Ir adatom: Symmetric structure

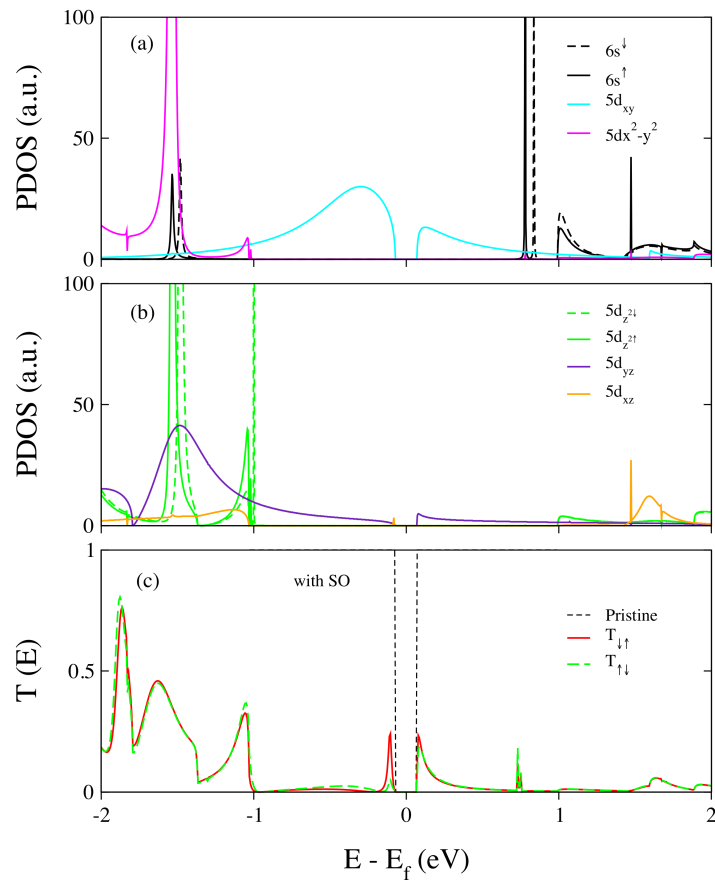


Figure S6: For Ir@AGNR-sy : (a)-(b) PDOS of polarized  $6s$  and  $5d$  orbitals of Ir. (c) Spin-flip transmission coefficients.

Fig. S6 shows a zoom in of the polarized PDOS for (a)  $6s$  and (b)  $5d$  orbitals of Ir. The transmission coefficients are also shown in chart (c) in order to highlight the eventual relation between the local impurity resonances with the energy states.